DALTON
FULL PAPER

Nickel complexes with tris(2-aminoethyl)amine (tren): $[Ni_3(tren)_4(H_2O)_2][Cr(ox)_3]_2\cdot 6H_2O$ (ox = oxalate), $\{[Ni_2(tren)_3][ClO_4]_4\cdot H_2O\}_n$, and $[Ni_2(tren)_2(aepd)][ClO_4]_4\cdot 2H_2O$ (aepd = *N*-(2-aminoethyl)pyrrolidine-3,4-diamine). Synthesis, structure and magnetism †

Vanessa M. Masters,[a] Paul V. Bernhardt,[a] Lawrence R. Gahan,*[a] Boujemaa Moubaraki,[b] Keith S. Murray[b] and Kevin J. Berry[c]

[a] *Department of Chemistry, The University of Queensland, Brisbane, QLD 4072, Australia*
[b] *Chemistry Department, Monash University, Clayton, Victoria 3168, Australia*
[c] *Westernport Secondary College, Hastings, Victoria 3915, Australia*

Received 2nd March 1999, Accepted 21st May 1999

Reaction of $K_3[Cr(ox)_3]$ (ox = oxalate) with nickel(II) and tris(2-aminoethyl)amine (tren) in aqueous solution resulted in isolation of the bimetallic assembly $[Ni_3(tren)_4(H_2O)_2][Cr(ox)_3]_2\cdot 6H_2O$. The polymeric complex $\{[Ni_2(tren)_3][ClO_4]_4\cdot H_2O\}_n$ has been prepared by reaction of nickel(II) perchlorate and tren in aqueous solution. From the same reaction mixture the complex $[Ni_2(tren)_2(aepd)][ClO_4]_4\cdot 2H_2O$ (aepd = *N*-(2-aminoethyl)pyrrolidine-3,4-diamine), in which a bridging tren ligand contains a carbon–carbon bond between two arms forming a substituted pyrrolidine, has been isolated. The complexes have been characterized by X-ray crystallography. The magnetic susceptibility (300–4.2 K) and magnetization data (2, 4 K, $H = 0$–5 T) for $\{[Ni_2(tren)_3][ClO_4]_4\cdot H_2O\}_n$ (300 K , 4.23 μ_B) exhibit evidence of weak antiferromagnetic coupling and zero field splitting ($2J = -1.8$ cm^{-1}; $|D| = 2$ cm^{-1}) at low temperature. For $[Ni_3(tren)_4(H_2O)_2][Cr(ox)_3]_2\cdot 6H_2O$ the susceptibility data at 300 K are indicative of uncoupled nickel(II) and chromium(III) sites with zero-field splitting and intramolecular antiferromagnetic coupling predicted at low temperature.

Introduction

Magnetic interactions between complex cations and anions, propagated by intermolecular effects such as those occurring though hydrogen bonded water molecules, might be expected to be weak.[1] For example, the complex $[Cu(tpm)_2]_3[Cr(ox)_3]_2\cdot 20H_2O$ ($S_1 = \frac{1}{2}$, $S_2 = \frac{3}{2}$; tpm = tris(pyrazolyl)methane; ox = oxalate) shows weak ferromagnetic coupling below 20 K.[1] However, the potential for variation in magnetic characteristics of both the complex cation and the complex anion makes the resulting possibility of ferro- or ferri-magnetic interactions attractive,[2] and the search for examples of bimetallic complexes of some interest.[1–5]

We have chosen to explore the synthesis of complex bimetallic salts of chromium(III) and nickel(II). Bimetallic complexes of this type have been reported, *e.g.* $[Cr(NH_3)_6][Ni(H_2O)_6]Cl_5\cdot \frac{1}{2}NH_4Cl$,[6] the interest being in the combination of $S = \frac{3}{2}$ and 1 spin states in octahedral fields.[7–10] In the present case $[Cr(ox)_3]^{3-}$ is employed as the complex anion and the complex cation results from the interaction of nickel(II) with tris(2-aminoethyl)-amine (tren). In addition, two complexes of tren with nickel(II) have been identified, the first the polymeric species $\{[Ni_2(tren)_3][ClO_4]_4\cdot H_2O\}_n$ and the second $[Ni_2(tren)_2(aepd)][ClO_4]_4\cdot 2H_2O$, in which a bridging tren ligand contains a carbon–carbon bond between two arms forming the substituted pyrrolidine (aepd = *N*-(2-aminoethyl)pyrrolidine-3,4-diamine).

Experimental

Materials

Tris(2-aminoethyl)amine (tren), classified as 96%, was obtained from Aldrich Chemical Company and either used without further purification or first distilled and fractionated. Samples of tren from two separate bottles were employed. For GC-MS a Hewlett Packard 5890 gas chromatograph, 5970 Series mass selective detector and a 25 m BPS column (0.25 mm i.d., 0.25 μm phase thickness) were employed. The temperature was raised from 100 to 270 °C at a rate of 16° min^{-1}; the oven was held at 100 °C for 2 min, raised at 16° min^{-1} to 270 °C, then held at that temperature for 10 min. Helium was used as carrier at a head pressure of 20 psi. ^{13}C-{^1H} NMR spectra were recorded with a JEOL GX400 spectrometer.

Syntheses

CAUTION: perchlorate salts of metal complexes are potentially explosive and should be handled in small quantities.

$[Ni_3(tren)_4(H_2O)_2][Cr(ox)_3]_2\cdot 6H_2O$. The salt $Ni(NO_3)_2\cdot 6H_2O$ (1.0 g; 3.44 mmol) was dissolved in a small volume of ethanol (10 cm^3) and tren (3 cm^3) was added dropwise until a lilac precipitate appeared. The mixture was filtered, and the product washed with ethanol (20 cm^3) diethyl ether (20 cm^3) and dried in air. The resulting purple solid was dissolved in water (20 cm^3) and an aqueous solution (5 cm^3) of $K_3[Cr(ox)_3]\cdot 3H_2O$ (0.56 g; 1.15 mmol) added. Ethanol (5 cm^3) was added slowly until the solution became cloudy, at which time water (1 cm^3) was added until the solution clarified. Within several hours small deep purple crystals suitable for X-ray crystallographic studies had formed (20 mg) (Found: C, 27.1; H, 5.84; N, 14.2. $[Ni_3(tren)_4(H_2O)_2][Cr(ox)_3]_2\cdot 6H_2O$ requires C, 28.1; H, 5.78 ; N, 14.6%).

$\{[Ni_2(tren)_3][ClO_4]_4\cdot H_2O\}_n$. The salt $Ni(ClO_4)_2\cdot 6H_2O$ (1.0 g; 2.73 mmol) dissolved in a small volume of ethanol (20 cm^3) and tren (3 cm^3; 0.02 mol) added dropwise. A lilac precipitate

† *Non-SI unit employed*: $\mu_B \approx 9.27 \times 10^{-24}$ J T^{-1}.

appeared immediately. The solution was filtered, and the product washed with ethanol and dried in air (1.60 g). The precipitate was dissolved in water (100 cm^3) and the solution left to stand on the bench. Lilac crystals, suitable for X-ray crystallographic studies, grew over a period of a week (0.5 g) (Found: C, 21.5; H, 5.9; N, 16.8. $\{[Ni_2(tren)_3][ClO_4]_4\cdot H_2O\}_n$ requires C, 22.2; H, 5.8; N, 17.3%). Small violet crystals which were separated manually were also observed (Found: C, 21.4; H, 5.7; N, 16.6. $[Ni_2(tren)_2(aepd)][ClO_4]_4\cdot 2H_2O$ requires C, 21.9; H, 5.7; N, 17.0%). The same products were obtained using tren which had been distilled and fractionated.

Crystallography

Data collection, structure solution and refinement. Cell constants were determined by a least-squares fit to the setting parameters of 25 independent reflections measured on an Enraf-Nonius CAD4 four circle diffractometer employing graphite monochromated Mo-Kα radiation (λ 0.71073 Å) and operating in the ω–2θ scan mode. Data reduction and empirical absorption corrections (ψ scans) were performed with the XTAL[11] package. Structures were solved by heavy atom methods with SHELXS 86[12] and refined by full-matrix least-squares analysis on F^2 with SHELXL 93.[13] All non-H atoms were refined with anisotropic thermal parameters except those mentioned below. Crystal data appear in Table 1. The atomic nomenclature is defined in Figs. 1–4 drawn with PLATON.[14]

Abnormal features. *$\{[Ni_2(tren)_3][ClO_4]_4\cdot H_2O\}_n$.* This polymeric structure exhibited disorder in the positions both the bridging and terminally bound tren ligands. The refined model comprised independent polymeric chains with occupancies restrained to 50%. The co-ordination sphere of Ni(1) comprises two monodentate bridging tren ligands, N(2*n*A)/C(2*n*A) and N(2*n*B)/C(2*n*B), in addition to a tetradentate terminally bound tren, N(1*n*)/C(1*n*). All of these ligands are disordered about the mirror plane upon which Ni(1) is situated. Centrosymmetrically related pairs of tridentate tren ligands are bound to Ni(2) in an alternating array along the chain, *i.e.* N(2*n*A)/C(2*n*A) : N(2*n*A)/C(2*n*A) then N(2*n*B)/C(2*n*B) : N(2*n*B)/C(2*n*B). The C and N atoms in these bridging ligands were refined with isotropic thermal parameters. Positional disorder in all ClO_4^- anions necessitated refinement of all O atoms with isotropic thermal parameters.

$[Ni_2(tren)_2(aepd)][ClO_4]_4\cdot 2H_2O$. The bridging *rac*-aepd ligand was found to exhibit disorder between its enantiomeric *RR* and *SS* isomers. The occupancies of the resulting diastereomeric complexes shown in Fig. 4 were 60 and 40% respectively. Perchlorate disorder was also identified in this structure and the O atoms connected to Cl(3) were refined with isotropic thermal parameters.

$[Ni_3(tren)_4(H_2O)_2][Cr(ox)_3]_2\cdot 6H_2O$. Two of the waters of crystallisation (O(15) and O(16)) were each disordered over three sites of occupancies of 40 : 40 : 20%.

CCDC reference number 186/1473.

See http://www.rsc.org/suppdata/dt/1999/2323/ for crystallographic files in .cif format.

Magnetic studies

Magnetic susceptibility measurements were made using a Quantum Design MPMS SQUID magnetometer with an applied field of 1 T. The powdered sample was contained in a calibrated gelatine capsule which was held in the centre of a drinking straw fixed to the end of the sample rod. For high-field magnetization work (0 to 5 T) the samples were also contained in the gelatine capsule. The magnetization values of the instrument were calibrated against a standard palladium sample, supplied by Quantum design, and also against chemical calibrants such as $CuSO_4\cdot 5H_2O$ and $[Ni(en)_3][S_2O_3]$ (en = ethylenediamine). Effective magnetic moments, per mol, were calculated using the relationship $\mu_{eff} = 2.828(\chi_m T)^{\frac{1}{2}}$ where χ_m is the susceptibility per mol of complex.

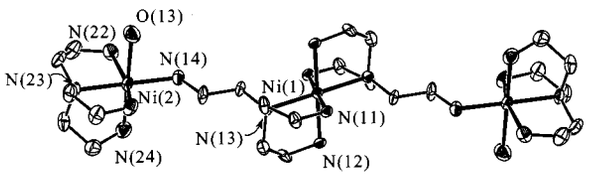

Fig. 1 A PLATON plot of the complex cation $[Ni_3(tren)_4(H_2O)_2]^{6+}$ with relevant atoms labelled; 30% probability ellipsoids are shown.

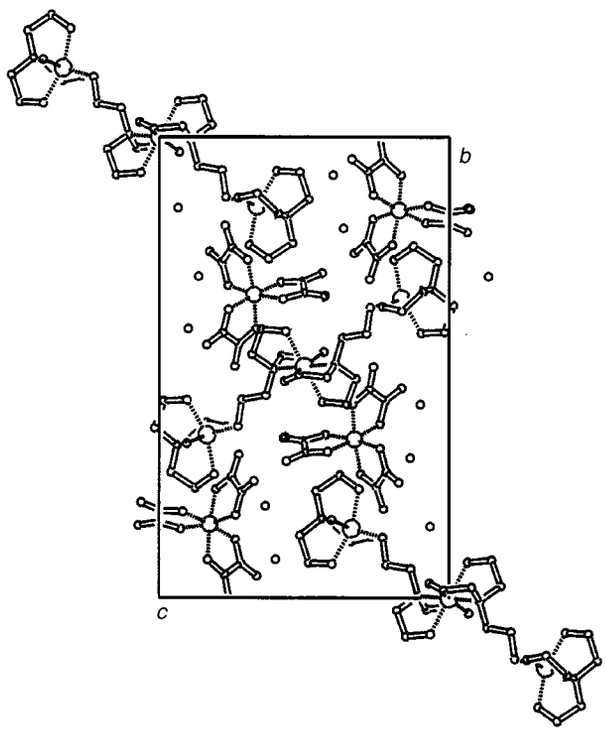

Fig. 2 Packing diagram for $[Ni_3(tren)_4(H_2O)_2][Cr(ox)_3]_2\cdot 6H_2O$.

Results and discussion

Crystal structures

Deep purple crystals of the complex double salt $[Ni_3(tren)_4(H_2O)_2][Cr(ox)_3]_2\cdot 6H_2O$ crystallized from aqueous solution after an excess of tren was treated with a nickel(II) salt and $K_3[Cr(ox)_3]$ added. The structure consists of a complex cation ($[Ni_3(tren)_4(H_2O)_2]^{6+}$), two complex anions ($[Cr(ox)_3]^{3-}$), and water molecules. The structure of the complex cation is depicted in Fig. 1 whilst Fig. 2 shows the packing diagram. Selected bond distances and angles are listed in Table 2.

The three nickel(II) ions in the $[Ni_3(tren)_4(H_2O)_2]^{6+}$ cation do not have the same co-ordination sphere. The central nickel(II) ion is situated at a centre of symmetry and is bonded to two facially co-ordinated tridentate tren ligands. Each tren ligand bears a pendant primary amine which is co-ordinated to a terminal nickel(II) ion. The terminal enantiomeric pair of octahedral nickel(II) ions are each bound to a single tetradentate tren ligand, a pendant amine from the central $Ni(tren)_2^{2+}$ unit, and an aqua ligand. Each of the nickel(II) ions exhibits a distorted octahedral geometry, with the angle between two *cis* nitrogen atoms (N–Ni–N) in the range 80.1–99.9°. The Ni–N bond lengths are in the range 2.052(9)–2.111(9) Å for the terminal nickel and 2.099(7)–2.152(8) Å for the central nickel. The Ni–N bond lengths for the terminal nickel ions in $[Ni_3(tren)_4(H_2O)_2]^{6+}$ were slightly different to the range observed for $[Ni(tren)Cl(H_2O)]Cl\cdot H_2O$ (2.047–2.172 Å).[15] The structure of the $[Cr(ox)_3]^{3-}$ anion is essentially the same as seen previously

Table 1 Crystal data for $[Ni_3(tren)_4(H_2O)_2][Cr(ox)_3]_2\cdot 6H_2O$, $\{[Ni_2(tren)_3][ClO_4]_4\cdot H_2O\}_n$ and $[Ni_2(tren)_2(aepd)][ClO_4]_4\cdot 2H_2O$

	$[Ni_3(tren)_4(H_2O)_2][Cr(ox)_3]_2\cdot 6H_2O$	$[Ni_2(tren)_2(aepd)][ClO_4]_4\cdot 2H_2O$	$\{[Ni_2(tren)_3][ClO_4]_4\cdot H_2O\}_n$
Empirical formula	$C_{36}H_{88}Cr_2N_{16}Ni_3O_{32}$	$C_{18}H_{56}Cl_4N_{12}Ni_2O_{18}$	$C_{18}H_{56}Cl_4N_{12}Ni_2O_{17}$
Formula weight	1537.35	987.97	971.97
T/K	293(2)	293(2)	293(2)
Crystal system	Monoclinic	Triclinic	Monoclinic
Space group	$P2_1/n$	$P\bar{1}$	$P2_1/m$
a/Å	9.0430(10)	9.968(2)	8.784(3)
b/Å	24.151(3)	15.480(1)	23.414(2)
c/Å	15.318(2)	15.684(2)	10.310(3)
α/°		118.552(7)	
β/°	96.619(7)	104.25(1)	108.06(1)
γ/°		97.47(1)	
V/Å^3	3323.1(7)	1971.5(5)	2016.0(9)
Z	2	2	2
D_c/g cm^3	1.536	1.664	1.601
μ/mm^{-1}	1.245	1.31	1.278
F(000)	1608	1032	1016
Reflections collected	6220	7353	3893
Independent reflections	5829 [R(int) = 0.0868]	6916 [R(int) = 0.0262]	3647 [R(int) = 0.0505]
Data/restraints/parameters	5829/0/411	6916/0/504	3647/0/311
Goodness of fit on F^2	1.005	1.02	1.048
Final $R1$, $wR2$ [$I > 2\sigma(I)$]	0.0775, 0.2013	0.0470, 0.1283	0.0902, 0.2435
(all data)	0.2008, 0.2746	0.0838, 0.1503	0.1990, 0.3210
Residual extrema/e Å^{-3}	0.952, −0.549	1.463, −0.577	1.683, −0.595

Table 2 Selected bond distances (Å) and bond angles (°) for $[Ni_3(tren)_4(H_2O)_2][Cr(ox)_3]_2\cdot 6H_2O$

Cr(1)–O(5)	1.959(7)	Cr(1)–O(1)	1.966(7)
Cr(1)–O(6)	1.971(7)	Cr(1)–O(2)	1.972(8)
Cr(1)–O(3)	1.975(7)	Cr(1)–O(4)	1.980(7)
C(1)–C(2)	1.57(2)	C(3)–C(4)	1.55(2)
C(5)–C(6)	1.55(2)	Ni(1)–N(12)	2.099(7)
Ni(1)–N(11)	2.139(8)	Ni(1)–N(13)	2.152(8)
Ni(2)–N(23)	2.088(9)	Ni(2)–N(22)	2.111(9)
Ni(2)–N(24)	2.089(11)	Ni(2)–N(21)	2.100(10)
Ni(2)–O(13)	2.229(9)	Ni(2)–N(14)	2.052(9)
O(5)–Cr(1)–O(1)	93.5(3)	O(5)–Cr(1)–O(6)	82.3(3)
O(1)–Cr(1)–O(6)	175.1(3)	O(5)–Cr(1)–O(2)	93.7(3)
O(1)–Cr(1)–O(2)	82.4(3)	O(6)–Cr(1)–O(2)	95.3(3)
O(5)–Cr(1)–O(3)	91.5(3)	O(1)–Cr(1)–O(3)	89.5(3)
O(6)–Cr(1)–O(3)	93.2(3)	O(2)–Cr(1)–O(3)	170.6(3)
O(5)–Cr(1)–O(4)	172.9(3)	O(1)–Cr(1)–O(4)	91.2(3)
O(6)–Cr(1)–O(4)	93.1(3)	O(2)–Cr(1)–O(4)	92.2(3)
O(3)–Cr(1)–O(4)	83.2(3)	N(12)–Ni(1)–N(11)	92.8(3)
N(12)–Ni(1)–N(13)	82.8(3)	N(11)–Ni(1)–N(13)	80.1(3)
N(14)–Ni(2)–N(23)	176.6(4)	N(14)–Ni(2)–N(24)	93.4(4)
N(23)–Ni(2)–N(24)	84.3(4)	N(14)–Ni(2)–N(21)	95.1(4)
N(23)–Ni(2)–N(21)	82.7(4)	N(14)–Ni(2)–N(22)	100.2(4)
N(24)–Ni(2)–N(21)	95.3(4)	N(24)–Ni(2)–N(22)	95.2(4)
N(23)–Ni(2)–N(22)	82.5(3)	N(14)–Ni(2)–O(13)	86.4(4)
N(21)–Ni(2)–N(22)	160.9(4)	N(24)–Ni(2)–O(13)	179.8(3)
N(23)–Ni(2)–O(13)	95.8(4)	N(22)–Ni(2)–O(13)	84.7(4)
N(21)–Ni(2)–O(13)	84.8(4)		

Table 3 Selected bond lengths (Å) and angles (°) for $\{[Ni_2(tren)_3][ClO_4]_4\cdot H_2O\}_n$

Ni(1)–N(11)	2.08(2)	Ni(1)–N(13)	2.11(2)
Ni(1)–N(12)	2.17(2)	Ni(1)–N(22A)	2.17(2)
Ni(1)–N(14)	2.22(3)	Ni(2)–N(24A)	2.09(2)
Ni(2)–N(23A)	2.13(2)	Ni(2)–N(22B)	2.14(2)
Ni(2)–N(21B)	2.14(2)	Ni(2)–N(24B)	2.14(2)
Ni(2)–N(21A)	2.16(2)		
N(11)–Ni(1)–N(23B^3)	99.7(10)	N(11)–Ni(1)–N(13)	80.5(7)
N(23B^2)–Ni(1)–N(13)	83.0(7)	N(11)–Ni(1)–N(12)	83.7(9)
N(13)–Ni(1)–N(12)	161.2(5)	N(13)–Ni(1)–N(22A)	102.2(8)
N(11)–Ni(1)–N(14)	83.0(11)	N(23B^2)–Ni(1)–N(14)	82.4(10)
N(23B^3)–Ni(1)–N(14)	177.2(11)	N(13)–Ni(1)–N(14)	98.1(8)
N(12)–Ni(1)–N(14)	90.1(9)	N(24A)–Ni(2)–N(23A)	92.3(8)
N(22B)–Ni(2)–N(21B)	84.3(7)	N(22B)–Ni(2)–N(24B)	93.6(9)
N(21B)–Ni(2)–N(24B)	81.9(7)	N(24A)–Ni(2)–N(21A)	82.2(7)
N(24A^3)–Ni(2)–N(21A)	97.8(7)	N(23A)–Ni(2)–N(21A)	81.9(7)

Symmetry relations: $^2 -x+1,\ y-\frac{1}{2},\ -z+1$. $^3 -x+1,\ -y+1,\ -z+1$.

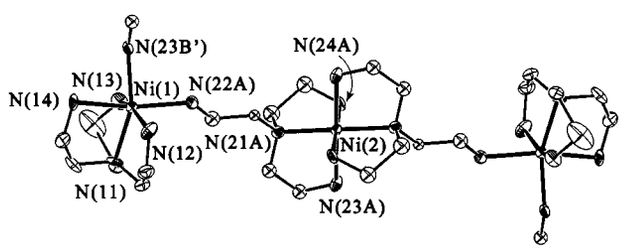

Fig. 3 A PLATON plot of the complex cation $[Ni_2(tren)_3]^{4+}$ with relevant atoms labelled; 30% probability ellipsoids are shown.

for $K_3[Cr(ox)_3]\cdot 3H_2O$.[16] The bimetallic complex has a number of waters of crystallization, two of which are disordered over three sites. The most notable hydrogen bonding interaction is that between a chelating oxygen of $[Cr(ox)_3]^{3-}$ and a water molecule co-ordinated to nickel(II) (O(4)···H(13B)–O(13) 2.179 Å, 174.8°). The distances Cr···Ni(2), Cr···Ni(1), and Ni(1)···Ni(2) are 7.618, 14.252 and 7.431 Å, respectively.

The complex $\{[Ni_2(tren)_3][ClO_4]_4\cdot H_2O\}_n$ consists of a polymeric cation, perchlorate anions and a water molecule. The structure of the cation $[Ni_2(tren)_3]^{4+}$ is depicted in Fig. 3, and selected bond distances and angles are listed in Table 3. There are two distinct geometries in which the nickel(II) ions in $\{[Ni_2(tren)_3][ClO_4]_4\cdot H_2O\}_n$ exist. In the first instance, two tren molecules act as tridentate ligands and co-ordinate to a single nickel ion, with each tren ligand having a pendant arm ending with a primary amine. In the second case, a single tren molecule co-ordinates to a single nickel(II) ion in a tetradentate fashion with the two remaining co-ordination sites occupied by the pendant primary amines from tren ligands bound tridentate to neighbouring nickel(II) ions. The $[Ni(tren)_2]^{2+}$ fragment is located on a centre of symmetry, but disordered over two positions. The $[Ni(tren)(RNH_2)_2]^{2+}$ moiety is situated on a mirror plane that passes through the atoms Ni(1), N(13), C(14) and C(15). However, this plane does not coincide with any local symmetry element of the complex, so all atoms in this fragment not lying on this mirror plane are disordered. These two disordered components comprise a pair of $[Ni(tren)(RNH_2)_2]^{2+}$ enantiomers. The centre of symmetry at Ni(2) results in an alternating array of the two enantiomeric $[Ni(tren)(RNH_2)_2]^{2+}$

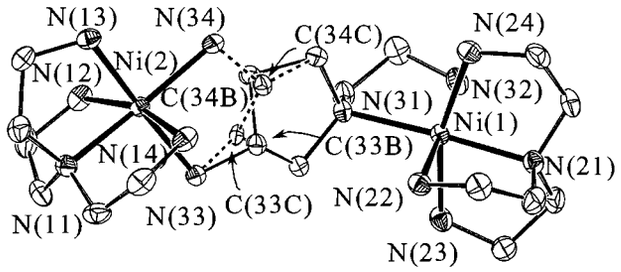

Fig. 4 A PLATON plot of the complex cation $[Ni_2(tren)_2(aepd)]^{4+}$ (*lel*, *ob*) with relevant atoms labelled; 30% probability ellipsoids are shown.

fragments along the polymer bridged by centrosymmetric $[Ni(tren)_2]^{2+}$ units. When disorder at both nickel(II) centres is considered, the polymeric structure may be separated into two similar, achiral strands, which are 'out of phase' with respect to the position of the enantiomeric $[Ni(tren)(RNH_2)_2]^{2+}$ moieties. Despite the disorder, the structures of $\{[Ni_2(tren)_3][ClO_4]_4\cdot H_2O\}_n$ and $[Ni_3(tren)_4(H_2O)_2][Cr(ox)_3]_2\cdot 6H_2O$ are actually quite similar. The cationic portion of the latter structure may be thought of as being derived from $\{[Ni_2(tren)_3][ClO_4]_4\cdot H_2O\}_n$ by terminating the polymeric chain with aqua ligands. Refinement in the more common acentric space group $P2_1$ was tried but this led to a worse *R* parameter and unreasonable interatomic distances and angles. All of the nickel ions are in a slightly distorted octahedral geometry with the angles between two *cis* N atoms (N–Ni–N) in the range 80.5(7)–98.1(7)°. The Ni–N distances are in the range 2.08–2.22(2) Å and the Ni···Ni separation is 7.5 Å.

Complexes of the type $[Ni_2(tren)_3]^{4+}$ or $[Ni(tren)_2]^{2+}$ have been reported,[17–19] and the $[Ni(tren)_2]^{2+}$ unit has been structurally characterized in the complexes $[Ni(tren)_2][BF_4]_2$ and $[Ni(tren)_2][Ni(mnt)_2]$ (mnt = maleonitriledithiolate dianion).[20] In both $[Ni(tren)_2][Ni(mnt)_2]$ and $[Ni(tren)_2][BF_4]_2$ the tridentate tren ligands are facially co-ordinated with pendant primary amines and the geometries of the cations are nearly identical with Ni–N bond lengths in the range 2.129(2)–2.172(2) Å,[20] although the bond lengths for the $Ni(tren)_2^{2+}$ centre of $Ni_3(tren)_4^{6+}$ are shorter than seen in $[Ni(tren)_2][BF_4]_2$.

The structure of $[Ni_2(tren)_2(aepd)][ClO_4]_4\cdot 2H_2O$ consists of the complex cation, four perchlorate anions and two water molecules. Fig. 4 shows a PLATON drawing of the cation which has two tren ligands bound in a tetradentate manner capping each metal ion. The two metal centres are joined by a bridging ligand which is an analogue of tren but has a carbon–carbon bond (1.50(2) Å, Table 4) joining two arms of the tren ligand, resulting in the substituted pyrrolidine, aepd.

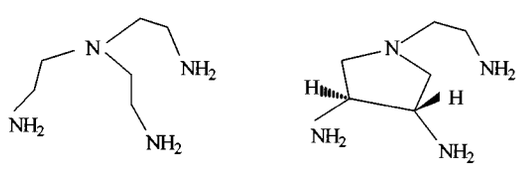

The geometries about each metal ion are that of a distorted octahedron with N–Ni–N angles in the range 81.2(3)–99.6(2)°. The octahedral environment about one nickel(II) site is composed of four nitrogen donors from a tren ligand and two primary amine donors in a five membered chelate ring formed by the pyrrolidine. The second nickel(II) site is again composed of a tetradentate tren ligand, the remaining two co-ordination sites occupied by a tertiary nitrogen donor from the pyrrolidine and the pendant primary amine from the 2-aminoethyl moiety. The Ni–N bond lengths associated with the tetradentate tren ligands lie within the range 2.087(7)–2.164(4) Å, a larger range than reported for other nickel(II) complexes of tren.[15,20–23] For the pyrrolidine ligand the Ni–N (primary amine) distances are significantly different (2.202(4) and 2.132(4) Å) with the Ni–N (tertiary) distance (2.165(4) Å) longer than that for the analogous bond in the capping tren ligands (2.087(4) and 2.103(4) Å). The complex crystallizes in diasteroisomeric forms, differentiated by the chirality around carbon atoms C(33) and C(34). The diasteroisomer can be differentiated by the conformations of C(33B)–C(34B)/C(33C)–C(34C) relative to C(13A)-C(13B) (*lel* 60%: *ob* 40%,[24] respectively). The distance between the two nickel ions is 6.79 Å.

Table 4 Selected bond lengths (Å) and angles (°) for $[Ni_2(tren)_2(aepd)][ClO_4]_4\cdot 2H_2O$

Ni(1)–N(21)	2.103(4)	Ni(1)–N(22)	2.118(4)
Ni(1)–N(23)	2.144(4)	Ni(1)–N(24)	2.164(4)
Ni(1)–N(31)	2.165(4)	Ni(1)–N(32)	2.143(4)
Ni(2)–N(11)	2.087(4)	Ni(2)–N(13)	2.096(4)
Ni(2)–N(14)	2.113(4)	Ni(2)–N(34)	2.132(4)
Ni(2)–N(12)	2.147(4)	Ni(2)–N(33)	2.202(4)
C(33B)–C(34B)	1.50(2)		
N(21)–Ni(1)–N(31)	177.3(2)	N(32)–Ni(1)–N(31)	82.7(2)
N(11)–Ni(2)–N(34)	177.3(2)	N(34)–Ni(2)–N(33)	83.0(2)

A ^{13}C-$\{^1H\}$ NMR spectrum of a concentrated sample of the commercial tren, recorded in $CDCl_3$, revealed two major resonances at δ 56.32 and 38.45 assigned to the methylene carbon atoms adjacent to the tertiary nitrogen and the primary amine of tren, respectively. Sets of lower intensity (<3%) resonances at δ 38.96, 57.87, 59.46 and 60.80 were also evident, with indications of even weaker resonances at δ 48.4, 51.52, 58.02, and 60.22. The DEPT spectra indicated that for the weaker signals the resonances at δ 38.96, 57.87 and 60.80 arose from methylene carbon atoms whilst that at δ 59.46 arose from a methine carbon suggesting that compounds such as aepd were possible contaminants. The GC-MS analysis of samples of tren also indicated the presence of a number of components, although they were poorly separated under the column conditions. The mass spectra of the two most significant components of the mixture corresponded to tren (M^+, *m*/*z* 147, calc. 146.24; *m*/*z* 129, 116, 112, 99, 87, 73 and 70) and a minor fraction with M^+ at *m*/*z* 145 which exhibited a mass spectral breakdown pattern identical to that of tren, but displaced by two mass units suggestive of, but not unambiguously assigned to, aepd (calc. for M^+, *m*/*z* 144.23; *m*/*z* 127, 114, 97, 85, 71 and 68). The chromatographic analysis indicated that the compounds with M^+ at *m*/*z* 145 and 147 had approximately the same boiling point, and subsequent distillation and fractionation of tren failed to remove the *m*/*z* 145 peak in the GC-MS. It would seem therefore that the origin of the aepd is from the commercial sample of tren, which is catalogued as of 96% purity.

Magnetic susceptibility

The magnetic properties of powder samples of $\{[Ni_2(tren)_3][ClO_4]_4\cdot H_2O\}_n$ and $[Ni_3(tren)_4(H_2O)_2][Cr(ox)_3]_2\cdot 6H_2O$ are reported in the form of effective magnetic moment per mol *versus* *T* plots measured in a field of 1 T (Figs. 5 and 6, respectively). For $\{[Ni_2(tren)_3][ClO_4]_4\cdot H_2O\}_n$ at 300 K the moment (4.23 μ_B) is essentially that expected (4.00–4.60 μ_B) for two uncoupled nickel(II) ions ($S = 1$, $g = 2.0$–2.3).[25] The μ_{eff} values decrease a little in the region 300 ($\mu_{eff} = 4.23$ μ_B, $\chi_m T = 2.23$ cm^3 K mol^{-1}) to 30 K ($\mu_{eff} = 4.03$ μ_B, $\chi_m T = 2.03$ cm^3 K mol^{-1}) and then drop more rapidly to $\mu_{eff} = 3.19$ μ_B (1.27 cm^3 K mol^{-1}) at 4.5 K. The decrease in μ_{eff} below 30 K is indicative of zero field splitting (*D*) and/or weak antiferromagnetic coupling (*J*) between the two nickel(II) ($S = 1$) centres. The small but gradual decrease in μ_{eff} above 30 K is due to weak antiferromagnetic coupling and second order Zeeman (N_α) effects.

Two approaches were used in order to explain the magnetic data. In the first the data were fitted using the expression for a classical-spin Heisenberg chain ($S = 1$),[26–28] based on a

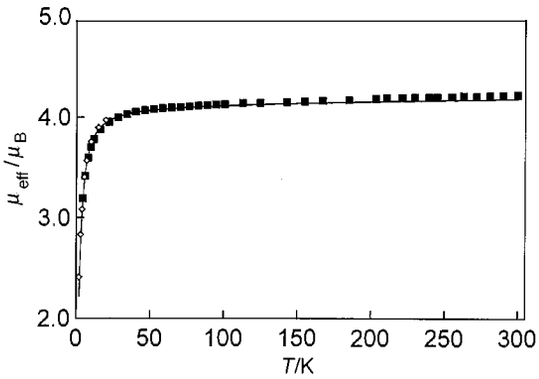

Fig. 5 Plot of μ_{eff} (per mol) *vs.* temperature for $\{[Ni_2(tren)_3][ClO_4]_4 \cdot H_2O\}_n$ measured in a field of 1 T. The solid line represents the best fit to the experimental data ($2J = -1.8$ cm^{-1}, $|D| = 2$ cm^{-1}, $g = 2.065$, $N_\alpha = 2.5 \times 10^{-4}$ cm^3 mol^{-1}); ■ from temperature *vs.* μ_{eff} data, ◇ from magnetization data.

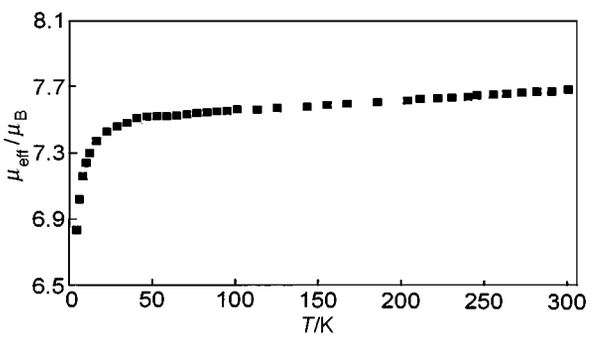

Fig. 6 Plot of μ_{eff} (per mol) *vs.* temperature for $[Ni_3(tren)_4(H_2O)_2][Cr(ox)_3]_2 \cdot 6H_2O$ measured in a field of 1 T.

$-JS_i \cdot S_{i+1}$ Hamiltonian (1) where $x = |J|/kT$ and the term N_α

$$\chi_m = \left(\frac{Ng^2\beta^2}{k(T-\theta)}\right)\left[\frac{2.0 + 0.0194x + 0.777x^2}{3.0 + 4.346x + 3.232x^2 + 5.834x^3}\right] + N_\alpha \quad (1)$$

accounting for temperature-independent paramagnetism, resulting in $J = -1.2$ cm^{-1}, θ (Weiss constant) $= -1.2$ K, $g = 2.28$, $N_\alpha = 5.0 \times 10^{-4}$ cm^3 mol^{-1} and $R = 6.1 \times 10^{-5}$ (the function minimized in curve fitting was $R = \Sigma\ (\chi_m^{obs} - \chi_m^{calc})^2/\Sigma\ (\chi_m^{obs})^2$). Calculations to incorporate the local anisotropy are neglected in this approach.[28] The g and N_α values are correlated to some extent and are a bit higher than normal. Incorporation of the small negative Weiss constant might imply the existence of very weak chain–chain interactions.

The second approach was an attempt to assess the contribution of both J and D to the low temperature susceptibility. Thus the polymer was considered in terms of the dimeric $[Ni_2(tren)_3]^{4+}$ moiety. The Hamiltonian (2) was employed.[28] The

$$\hat{H} = -2J\hat{S}_1 \cdot \hat{S}_2 + D(\hat{S}_1^2 + \hat{S}^2) + g\beta H \cdot S \quad (2)$$

energies of the ground state manifold for a dinuclear nickel(II) moiety were obtained by diagonalization of the appropriate 9×9 matrix under the above Hamiltonian operator. We have assumed that the g and D values of the two metal ions are the same even though the symmetries are different (Fig. 3). Further, the g values were assumed to be isotropic. The temperature dependence of the magnetic susceptibilities was calculated using the thermodynamic expression for the susceptibility rather than the Van Vleck equation.[28–30] This is particularly important for the low temperature magnetisation data, described below. A temperature independent susceptibility term (N_α) was also included;[28] J, D, and g were permitted to vary for best fit and N_α was set at 2.5×10^{-4} cm^3 mol^{-1}, which is the

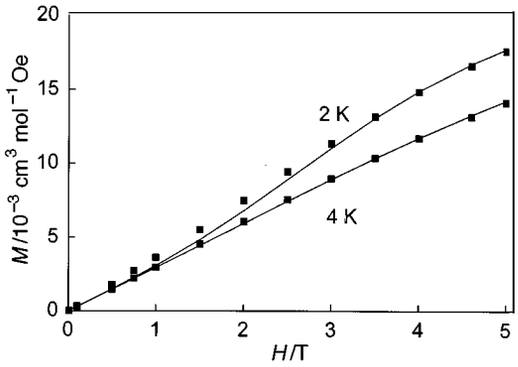

Fig. 7 Plots of magnetization M, *vs* field H for $\{[Ni_2(tren)_3][ClO_4]_4 \cdot H_2O\}_n$. Solid lines are calculated using $2J = -1.8$ cm^{-1}, $|D| = 2$ cm^{-1} and $g = 2.065$ (see text).

normal value for two mols of Ni^{II}.[27] A very good fit, shown in Fig. 5, was obtained for the following parameter set: $-g = 2.06$, $2J = -1.8$ cm^{-1} and $D = 2.0$ cm^{-1}. This set of parameter values was strongly supported when they were used to generate plots of magnetization *versus* applied field, in fields of 0 to 5 T. In Fig. 7 it can be seen that the 4 K data are very well simulated, as are the 2 K data in terms of the gentle S-shape, but with small discrepancies at intermediate field values. If J or D are set to zero there are large differences between observed and calculated magnetization plots. The g value obtained by matrix diagonalization is slightly less than normal values for Ni^{II} (2–2.1) while that obtained from the chain model (2.28) is high because of correlation effects and limitations of this chain model.

Whichever of the two approaches is employed suggests that the two nickel(II) sites are weakly antiferromagnetically coupled through the diamagnetic atoms joining them (Ni · · · Ni 7.5 Å). There are no significant intermolecular Ni · · · Ni pathways evident from the crystal structure and so the θ value obtained from the chain model, if real, may relate to dipolar effects. There are a number of reported instances of polynuclear nickel(II) complexes in which weak antiferromagnetic coupling occurs through diamagnetic bridges and these can be compared to the present system.[26,31–33]

For $[Ni_3(tren)_4(H_2O)_2][Cr(ox)_3]_2 \cdot 6H_2O$, the $\chi_m T$ values (per mol) in the region 300 ($\mu = 7.70$ μ_B, $\chi_m T = 7.41$ cm^3 K mol^{-1}) to 30 K ($\mu = 7.46$ μ_B, $\chi_m T = 6.96$ cm^3 K mol^{-1}) decrease a little in a linear fashion (Fig. 6). At 300 K for uncoupled nickel(II) and chromium(III) ions $\{3\mu_{eff}^2\ [Ni_3(tren)_4(H_2O)_2]^{6+} + 2\mu_{eff}^2\ [Cr(ox)_3]^{3-}\}$ the theoretical effective magnetic moment is 7.35 μ_B (S = 1, $\frac{3}{2}$, $g = 2$).[34] The value of $\chi_m T$ decreases rapidly below 30 K ($\mu = 6.83$ μ_B, $\chi_m T = 5.84$ cm^3 K mol^{-1}, 4.5 K). The general slope of the curve is similar to that in Fig. 5 for the $[Ni_2(tren)_3]^{4+}$ complex. The magnetic behaviour is also similar to that reported for the double salt $[Cu(tpm)_2]_3[Fe(ox)_3]_2 \cdot 20H_2O$ with μ_{eff} (300 K) 9.85 μ_B with Curie like behaviour between 300 and 4 K and weak antiferromagnetic coupling and/or zero field splitting at low temperature.[1] Contrastingly $[Cu(tpm)_2]_3[Cr(ox)_3]_2 \cdot 20H_2O$ exhibits Curie like behaviour between 300 and 20 K and weak ferromagnetic coupling below 20 K, the Cr^{III} · · · Cr^{III} interactions being mediated by hydrogen bonding of water to neighbouring oxalate groups. The intermolecular contacts include an interaction between a chelating oxygen of an oxalate ligand and a water molecule (O(1) · · · O(w) 2.90(1) Å),[1] similar to that observed for $[Ni_3(tren)_4(H_2O)_2][Cr(ox)_3]_2 \cdot 6H_2O$ (O(4) · · · H(13B)–O(13) 2.179 Å, 174.8°). Thus the weak antiferromagnetic behaviour of $[Ni_3(tren)_4(H_2O)_2][Cr(ox)_3]_2 \cdot 6H_2O$ could arise either from intramolecular coupling within the $Ni_2(tren)_3$ moiety and zero Ni · · · Cr coupling, or intermolecular interaction between $[Cr(ox)_3]^{3-}$ species as discussed above. Zero-field splitting from both the cation and, to a lesser extent, the anionic centres will contribute to the decrease occur-

ring below 30 K. In view of these ambiguities quantitative analysis was not pursued.

Concluding remarks

The isolation of the polymeric $\{[Ni_2(tren)_3][ClO_4]_4 \cdot H_2O\}_n$ complex and the bimetallic species $[Ni_3(tren)_4(H_2O)_2][Cr(ox)_3]_2 \cdot 6H_2O$ although unanticipated is, in retrospect, not surprising. Complexes of the type $[Ni_2(tren)_3]^{4+}$ or $[Ni(tren)_2]^{2+}$ have been reported previously, and indeed the results of a potentiometric titration of tren in the presence of nickel(II) can be fitted using a model which includes species such as $[Ni(tren)_2]^{2+}$ and $[Ni(tren)(Htren)]^{3+}$.[35] Further, the weak magnetic interactions observed appear typical for these types of complexes. However, the isolation of $[Ni_2(tren)_2(aepd)][ClO_4]_4 \cdot 2H_2O$ was remarkable given the previous extensive chemistry of tren and nickel(II)–tren systems. It is possible that the ligand has always been present in reaction mixtures, albeit in small amounts, but it presumably cannot compete with the strongly co-ordinating tetradentate tren. In the present case, an apparently ideal combination of tetradentate co-ordinating tren ligands coupled with the bridging bis-didentate aepd, which cannot bind to the same metal ion through more than two nitrogen atoms because of stereochemical constraints enforced by the pyrrolidine ring, results in the observed dinuclear nickel(II) hexaamine.

Acknowledgements

The financial support of the Australian Research Council is gratefully acknowledged.

References

1 K. S. Murray, G. D. Fallon, D. C. R. Hockless, K. D. Lu, B. Moubaraki and K. Van Langenberg, *ACS Symp. Ser.*, 1996, **644**, 201.
2 M. C. Morón, F. Palacio, J. Pons, J. Casabó, X. Solans, K. E. Merabet, D. Huang, X. Shi, B. K. Teo and R. L. Carlin, *Inorg. Chem.*, 1994, **33**, 746.
3 R. L. Carlin, *Comments Inorg. Chem.*, 1991, **11**, 215.
4 S. Decurtins, H. W. Schmalle, P. Schneuwly and H. R. Oswald, *Inorg. Chem.*, 1993, **32**, 1888.
5 V. A. Grillo, L. R. Gahan, G. R. Hanson and T. W. Hambley, *Polyhedron*, 1996, **15**, 559.
6 M. C. Morón, A. Le Bail and J. Pons, *J. Solid State Chem.*, 1990, **88**, 498.
7 Y. Pei, Y. Journaux and O. Kahn, *Inorg. Chem.*, 1989, **28**, 100.
8 T. Mallah, C. Auberger, M. Verdaguer and P. Veillet, *J. Chem. Soc., Chem. Commun.*, 1995, 61.
9 V. Gadet, T. Mallah, I. Castro and M. Verdaguer, *J. Am. Chem. Soc.*, 1992, **114**, 9213.
10 A. P. Ginsberg, *Inorg. Chim. Acta Rev.*, 1971, **5**, 45.
11 S. R. Hall, H. D. Flack and J. M. Stewart (Editors), *The XTAL3.2 User's Manual*, Universities of Western Australia, Geneva and Maryland, 1992.
12 G. M. Sheldrick, *Acta Crystallogr., Sect. A*, 1990, **46**, 467.
13 G. M. Sheldrick, SHELXL 93, A program for crystal structure determination, University of Göttingen, 1993.
14 A. L. Spek, PLATON, A Thermal ellipsoid plotting program, University of Utrecht, 1994.
15 A. Marzotto, D. A. Clemente and G. Valle, *Acta Crystallogr., Sect. C*, 1993, **49**, 1252.
16 D. Taylor, *Aust. J. Chem.*, 1978, **31**, 1455.
17 F. G. Mann, *J. Chem. Soc.*, 1929, 409.
18 F. G. Mann and W. J. Pope, *J. Chem. Soc.*, 1926, 482.
19 C. K. Jørgensen, *Acta Chem. Scand.*, 1956, **10**, 887.
20 G. J. Colpas, M. Kumar, R. O. Day and M. J. Maroney, *Inorg. Chem.*, 1990, **29**, 4779.
21 M. Salah El Fallah, E. Rentschler, A. Caneschi, R. Sessoli and D. Gatteschi, *Angew. Chem., Int. Ed. Engl.*, 1996, **35**, 1947.
22 R. D. Willett, *Acta Crystallogr., Sect. C*, 1987, **43**, 1494.
23 M. L. Calatayud, I. Castro, J. Sletten, J. Cano, F. Lloret, J. Faus, M. Julve, G. Seitz and K. Mann, *Inorg. Chem.*, 1996, **35**, 2858.
24 The *lel* and *ob* nomenclature is described in *Inorg. Chem.*, 1970, **9**, 1.
25 M. Ohba, N. Fukita and H. Ōkawa, *J. Chem. Soc., Dalton Trans.*, 1997, 1733.
26 H. L. Shyu, H. H. Wei and Y. Wang, *Inorg. Chim. Acta*, 1997, **258**, 81.
27 A. Meyer, A. Gleizes, J.-J. Girerd, M. Verdaguer and O. Kahn, *Inorg. Chem.*, 1982, **21**, 1729.
28 O. Kahn, *Molecular Magnetism*, VCH, New York, 1993, p. 257.
29 K. S. Murray, *Adv. Inorg. Chem.*, 1995, **43**, 261.
30 J. Glerup, P. A. Goodson, D. J. Hodgson and K. Michelson, *Inorg. Chem.*, 1995, **34**, 6255.
31 Y. Journaux, J. Sletten and O. Kahn, *Inorg. Chem.*, 1986, **25**, 439.
32 P. Chaudhuri, M. Winter, B. P. C. Della Vdova, E. Bill, A. Trautwein, S. Gehring, P. Fleischhauer, B. Nuber and J. Weiss, *Inorg. Chem.*, 1991, **30**, 2148.
33 R. Ruiz, M. Julve, J. Faus, F. Lloret, M. C. Muñoz, Y. Journaux and C. Bois, *Inorg. Chem.*, 1997, **36**, 3434.
34 L. N. Mulay, *Magnetic Susceptibility*, Interscience Publishers, New York, 1963, p. 1751.
35 L. R. Gahan and V. M. Masters, unpublished work.

Paper 9/01659G